

# Coulomb blockade double-dot Aharonov-Bohm interferometer: harmonic decomposition of the interference pattern

Feng Li,<sup>1</sup> HuJun Jiao,<sup>1</sup> Hui Wang,<sup>2</sup> JunYan Luo,<sup>3</sup> and Xin-Qi Li<sup>1,4</sup>

<sup>1</sup>State Key Laboratory for Superlattices and Microstructures, Institute of Semiconductors, Chinese Academy of Sciences, P.O. Box 912, Beijing 100083, China

<sup>2</sup>Department of Mathematics and Physics, China University of Petroleum, Beijing 102249, China

<sup>3</sup>Department of Chemistry, Hong Kong University of Science and Technology, Kowloon, Hong Kong

<sup>4</sup> Department of Physics, Beijing Normal University, Beijing 100875, China

(Dated: November 29, 2018)

For the solid state double-dot interferometer, the phase shifted interference pattern induced by the interplay of inter-dot Coulomb correlation and multiple reflections is analyzed by harmonic decomposition. Unexpected result is uncovered, and is discussed in connection with the which-path detection and electron loss.

PACS numbers: 73.23.-b, 73.23.Hk, 05.60.Gg

*Introduction.*— As an analogue of Young’s double-slit interference [1], a ring-like Aharonov-Bohm (AB) interferometer with a quantum dot in one of the interfering paths is of interest for many fundamental reasons and receives extensive studies [2, 3, 4, 5]. Very recently, an elegant study was further carried out for the closed-loop setup, with particular focus on the multiple-reflection induced inefficient which-path information by a nearby charge detector [6].

In this report we consider an alternative solid-state AB interferometer, say, electron transport through parallel double dots (DD) in Coulomb blockade regime, as schematically shown in Fig. 1. Existing studies on this DD setup include the cotunneling interference [7, 8, 9, 10], and two-loops (two fluxes) interference with the two dots as an artificial molecule [11, 12]. In this work we restrict to the DD *without* tunnel-coupling between the dots, which enables us to focus on the interplay of Coulomb correlation and quantum interference.

At first sight, this electronic setup looks similar to the double-slit interferometer [1]. Nevertheless, the underlying solid-state specifics will result in such novel behavior as non-analytic current switching tuned by very weak magnetic field [13]. In present work, we extend our previous study [13] to more general situations for off-resonant DD levels, in the presence of which-path detection and lossy channels. We find the interference pattern to be *asymmetric* with respect to the magnetic field, and attribute it to the underlying Coulomb correlations. Moreover, similar to Ref. 6, we present an analysis of harmonic decomposition for the interference pattern. We find that the phase shifts of the harmonic components of current are linearly scaled with the order of harmonics, and the high-order harmonics, in contrast to Ref. 6, will be dephased by the which-path detection.

*Model and Method.*— Consider the double dots connected in parallel to two leads. For simplicity we assume that in each dot there is only one level,  $E_{1(2)}$ , involved in the transport. Also, we neglect the spin degrees of freedom. In the case of strong Coulomb blockade, the effect of spin can be easily restored by doubling the tun-

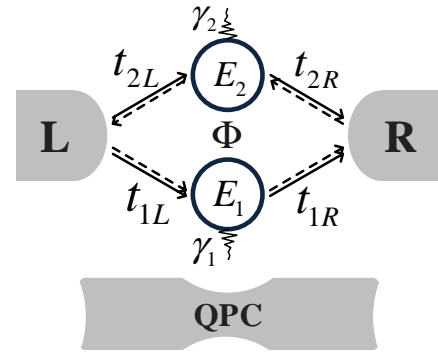


FIG. 1: Schematic setup of a double-dot Aharonov-Bohm interferometer. The solid-line trajectory is the usual first-order harmonic interference, while the dashed-line trajectory represents contribution to higher(second)-order harmonic interference. To address dephasing and electron-loss effects, a nearby quantum-point-contact (QPC) detector and lossy channels to side-reservoirs (with rates  $\gamma_{1(2)}$ ) are introduced.

neling rates of each QD with the left lead. The system is described by the following Hamiltonian

$$H = H_0 + H_T + \sum_{\mu=1,2} E_{\mu} d_{\mu}^{\dagger} d_{\mu} + U d_1^{\dagger} d_1 d_2^{\dagger} d_2. \quad (1)$$

Here the first term,  $H_0 = \sum_k [E_{kL} a_{kL}^{\dagger} a_{kL} + E_{kR} a_{kR}^{\dagger} a_{kR}]$ , describes the leads and  $H_T$  describes their coupling to the dots,

$$H_T = \sum_{\mu,k} \left( t_{\mu L} d_{\mu}^{\dagger} a_{kL} + t_{\mu R} a_{kR}^{\dagger} d_{\mu} \right) + \text{H.c.}, \quad (2)$$

where  $\mu = 1, 2$  and  $a_{kL}^{\dagger}$  and  $a_{kR}^{\dagger}$  are the creation operators for the electrons in the leads while  $d_{1,2}^{\dagger}$  are the creation operators for the DD. The last term in Eq. (1) describes the interdot repulsion. We assume that there is no tunnel coupling between the dots and that the couplings of the dots to the leads,  $t_{\mu L(R)}$ , are independent of energy.

In the absence of a magnetic field one can always choose the gauge in such a way that all couplings are real. In the presence of a magnetic flux  $\Phi$ , however, the tunneling amplitudes between the dots and the leads are in general complex. We write  $t_{\mu L(R)} = \bar{t}_{\mu L(R)} e^{i\phi_{\mu L(R)}}$ , where  $\bar{t}_{\mu L(R)}$  is the coupling without the magnetic field. The phases are constrained to satisfy  $\phi_{1L} + \phi_{1R} - \phi_{2L} - \phi_{2R} = \phi$ , where  $\phi \equiv 2\pi\Phi/\Phi_0$ .

To account for dephasing effect, we introduce a which-path detection by a nearby quantum point contact (QPC)[4], with a model description as in Ref. 14. To make contact with conventional double-slit interferometer, we also introduce electron lossy channels. Slightly differing from Ref. 5, instead of the semi-infinite tight binding chain introduced there, we model the lossy channels by attaching each dot with an electronic side-reservoir, which is particularly suited in the master equation approach. The side-reservoir model was originally proposed by Büttiker in dealing with phase-breaking effect [15], i.e., electron would lose phase information after entering the reservoir first, then returning back from it. But here, we assume that the reservoir's Fermi level is much lower than the dot energy. As a result, electron only enters the reservoir *unidirectionally*, never coming back.

The transport properties of the above described system can be conveniently studied by the number-resolved master equation [16, 17, 18]. The central quantity of this approach is the number-conditioned reduced state,  $\rho^{(n)}(t)$  of the double dots, where  $n$  is the electron number passed through the junction between the DD and an assigned lead where number counting is performed. Very usefully,  $\rho^{(n)}(t)$  is related to the electron-number distribution function, in terms of  $P(n, t) = \text{Tr}[\rho^{(n)}(t)]$ , where the trace is over the DD states. From  $P(n, t)$  the current and its fluctuations can be readily obtained. For current, for instance, it simply reads  $I(t) = ed\langle n(t) \rangle / dt$ , where  $\langle n(t) \rangle = \sum_n nP(n, t)$ . In practice, instead of directly solving  $P(n, t)$ , much simpler equation-of-motion technique is available for the calculation of current and current fluctuations [17, 18].

In large bias sequential tunnelling regime and under inter-dot Coulomb blockade (i.e. the DD can be occupied at most by one electron), the Hilbert space of the DD is reduced to  $|0\rangle \equiv |00\rangle$ ,  $|1\rangle \equiv |10\rangle$ , and  $|2\rangle \equiv |01\rangle$ , where  $|10\rangle$  means the upper dot occupied and the lower dot unoccupied, and other states have similar interpretations. Following Ref. 18, the “ $n$ ”-resolved master equation in this basis can be straightforwardly carried out as

$$\dot{\rho}_{00}^{(n)} = -2\Gamma_L \rho_{00}^{(n)} + (\gamma + \Gamma_R) \rho_{11}^{(n-1)} + (\gamma + \Gamma_R) \rho_{22}^{(n-1)} + e^{i(\phi_{R1} - \phi_{R2})} \Gamma_R \rho_{12}^{(n-1)} + e^{i(\phi_{R2} - \phi_{R1})} \Gamma_R \rho_{21}^{(n-1)} \quad (3a)$$

$$\dot{\rho}_{11}^{(n)} = \Gamma_L \rho_{00}^{(n)} - (\gamma + \Gamma_R) \rho_{11}^{(n)} - \frac{1}{2} e^{i(\phi_{R1} - \phi_{R2})} \Gamma_R \rho_{12}^{(n)} - \frac{1}{2} e^{i(\phi_{R2} - \phi_{R1})} \Gamma_R \rho_{21}^{(n)} \quad (3b)$$

$$\dot{\rho}_{22}^{(n)} = \Gamma_L \rho_{00}^{(n)} - (\gamma + \Gamma_R) \rho_{22}^{(n)} - \frac{1}{2} e^{i(\phi_{R1} - \phi_{R2})} \Gamma_R \rho_{12}^{(n)} - \frac{1}{2} e^{i(\phi_{R2} - \phi_{R1})} \Gamma_R \rho_{21}^{(n)} \quad (3c)$$

$$\dot{\rho}_{12}^{(n)} = e^{i(\phi_{L1} - \phi_{L2})} \Gamma_L \rho_{00}^{(n)} - \frac{1}{2} e^{i(\phi_{R2} - \phi_{R1})} \Gamma_R \rho_{11}^{(n)} - \frac{1}{2} e^{i(\phi_{R2} - \phi_{R1})} \Gamma_R \rho_{22}^{(n)} - \frac{1}{2} (\gamma_d + 2\gamma + 2i\Delta + 2\Gamma_R) \rho_{12}^{(n)} \quad (3d)$$

$$\dot{\rho}_{21}^{(n)} = e^{i(\phi_{L2} - \phi_{L1})} \Gamma_L \rho_{00}^{(n)} - \frac{1}{2} e^{i(\phi_{R1} - \phi_{R2})} \Gamma_R \rho_{11}^{(n)} - \frac{1}{2} e^{i(\phi_{R1} - \phi_{R2})} \Gamma_R \rho_{22}^{(n)} - \frac{1}{2} (\gamma_d + 2\gamma - 2i\Delta + 2\Gamma_R) \rho_{21}^{(n)} \quad (3e)$$

Here  $\dot{\rho}^{(n)}$  denotes the time derivative of the “ $n$ ”-conditional DD state. Owing to the neglected spin degrees of freedom in constructing the Hilbert space, as a compensation, we have replaced  $\Gamma_L$  with  $2\Gamma_L$  to equivalently restore the spin effect. In the above equations,  $\Delta = E_1 - E_2$  is the disalignment of the DD levels.  $\Gamma_{L(R)} = 2\pi D_{L(R)} |t_{L(R)}|^2$ , and  $\gamma_{1(2)} = 2\pi D_{1(2)} |t_{1(2)}|^2$ , are the respective coupling rates of the DD to the left and right leads, as well as to the side reservoirs.  $D_{L(R)}$  and  $D_{1(2)}$  are the density of states of the leads and reservoirs, while  $t_{L(R)}$  and  $t_{1(2)}$  are the respective tunneling

amplitudes. For simplicity, in this work we assume that  $\gamma_1 = \gamma_2 = \gamma$ , and  $\Gamma_L = \Gamma_R = \Gamma$  in the following numerical results. Finally,  $\gamma_d$  is the dephasing rate between the two dots, caused by the which-path measurement of QPC [14].

*Phase-Locking Breaking.*— In the absence of electron loss, i.e.,  $\gamma = 0$ , simple expression for the steady-state current is extractable:

$$I = \left\{ \frac{2(\gamma_d + 2\Gamma_R)(1 - \cos \phi) - 4\Delta \sin \phi}{\gamma_d(\gamma_d + 2\Gamma_R) + 4\Delta^2} + \frac{1}{I_0} \right\}^{-1}, \quad (4)$$

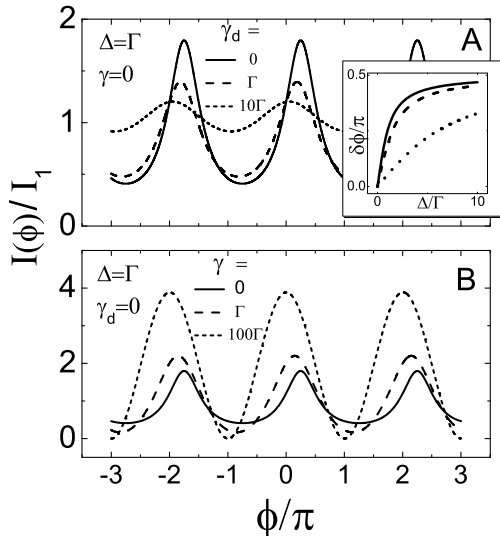


FIG. 2: (A) Phase shifted Aharonov-Bohm interference pattern, as a consequence of the interplay of Coulomb correlation and quantum coherence. Inset: shift of current peak *versus* the level detuning  $\Delta$ . Effect of dephasing between the two dots is demonstrated by varying  $\gamma_d$ . (B) Effect of electron loss. With increasing the lossy strength  $\gamma$ , conventional double-slit interference pattern is eventually restored.

where  $I_0 = 4\Gamma_L\Gamma_R/(4\Gamma_L + \Gamma_R)$ , is the current in the absence of magnetic flux. However, in the following we will use the current of transport through a Coulomb-blockade single dot,  $I_1 = 2\Gamma_L\Gamma_R/(2\Gamma_L + \Gamma_R)$ , to scale the double-dot current, in order to highlight the interference features.

In the absence of dephasing,  $\gamma_d=0$ , from Eq. (4) we have  $I = I_0\Delta^2/\{\Delta^2 + I_0[\Gamma_R(1 - \cos\phi) - \Delta\sin\phi]\}$ . Then a remarkable switching effect follows this result: as  $\Delta \rightarrow 0$ ,  $I = I_0$  for  $\phi = 2\pi n$ , while  $I = 0$  for any deviation of  $\phi$  from these values. Detailed interpretation for this novel behavior using a  $SU(2)$  transformation is referred to Ref. 13.

If  $\Delta \neq 0$ , the Coulomb correlation is manifested in an alternative way, see Fig. 2(A), where the current peaks deviate from  $\phi = 2\pi n$ . For small  $\Delta$ , we find that the current is peaking at  $\phi \approx \Delta/\Gamma_R + 2\pi n$ , and with a magnitude  $I_{\max} \approx (1/I_0 - 1/2\Gamma_R)^{-1}$ . Increasing  $\Delta$ , the current peak moves rightward. This kind of peak shift implies nothing but the symmetry breaking with respect to the magnetic-field inversion. This behavior contrasts with the following statement [19]: based on current conservation and time-reversal invariance, the Onsager relation, say, the symmetry relation of transport coefficients under inversion of magnetic field, will lock the current peaks at  $\phi = 2\pi n$ , for *any two-terminal linear transport*. This is usually referred to as *phase locking*. Beyond linear response, however, phase locking does not necessarily hold in general.

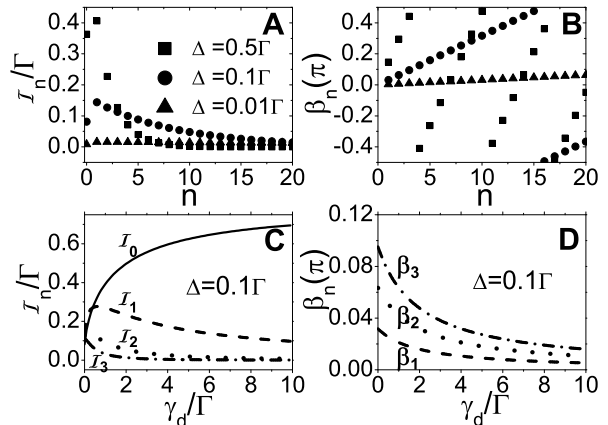


FIG. 3: Harmonic decomposition of the interference current  $I(\phi)$ . (A) and (B): Amplitude  $\mathcal{I}_n$  and phase shift  $\beta_n$  of the  $n$ -th harmonic component, for different energy detuning  $\Delta$ . In (B) an excellent linear-scaling relation for the phase shift, say,  $\beta_n = n\beta_1$ , is observed. (C) and (D): Effect of which-path detection on individual harmonic components. In contrast to Ref. 6, here the higher order harmonic components are also dephased (even more seriously). Interestingly, from (D) we find that the scaling relation  $\beta_n = n\beta_1$  still holds even in the presence of dephasing.

In Ref. 9, for instance, for the AB setup with a single dot embedded in one of the arms, it was found that the phase locking is indeed broken under finite bias voltage and *only* in the presence of electron-electron interaction. However, for the similar interacting DD system as considered here, breaking of phase locking was not found under finite bias voltage, in the case of  $\Delta = 0$  and within the cotunneling transport mechanism [9]. Here, we find that the current is asymmetric *only* for  $\Delta \neq 0$ , while it is still symmetric for  $\Delta = 0$ , being somewhat in agreement with Ref. 9, despite the different transport mechanism and dephasing involved here.

*Dephasing and Lossy Effects.*— In Fig. 2(A), we also observe that the current at  $\phi = 2\pi n$  is not affected by  $\Delta$  and  $\gamma_d$ . This feature implies that the current in case of complete dephasing is the same as the one from constructive interference (i.e. with  $\phi = 2\pi n$ ), being different from the conventional double-slit interference [1]. We attribute this feature to the closed boundary condition, under which the multiple reflection plays essential role. By introducing lossy channels, i.e., allowing electron loss from the DD to surrounding environment, in Fig. 2(B) we see that all these features disappear and the conventional double-slit interference pattern is restored by increasing the lossy rate  $\gamma$ . The reason is that, as the dots become more and more open, the side reservoirs would reduce the occupation probability on the dots, thus make the Coulomb correlation and back-reflection less important.

*Harmonic Decomposition.*— To highlight the effect of the closed nature and Coulomb correlation, we fur-

ther expand Eq. (4) into Fourier series,  $I(\phi) = \mathcal{I}_0 + \sum_{n=1}^{\infty} \mathcal{I}_n \cos(n\phi + \beta_n)$ . Physically, the  $n$ -th order harmonic stems from trajectories which have  $n$ -turns difference surrounding the magnetic flux between the two interfering partial waves (see Fig. 1). In Fig. 3 (A) and (B), we plot the amplitude  $\mathcal{I}_n$  and phase shift  $\beta_n$  for coherent case. The higher order harmonics are caused by the multiple reflections under closed boundary condition, while the phase shift is related to Coulomb correlation between the two dots (note that there is no phase shift for noninteracting DD). Quite surprisingly, in Fig. 3(B) we observe that  $\beta_n = n\beta_1$ . At this stage, unfortunately, we failed to find a satisfied interpretation for this interesting result, so would remain it for future study.

In Fig. 3 (C) and (D), dephasing effect is shown. Note that, as explained in the model description, in this work dephasing is modelled by a *which-path* detection. Interestingly, we observe here that the which-path detection also dephases the higher order harmonic components of current, unlike in Ref. 6, where only the first-harmonic amplitude is strongly reduced by the detection, while the second one is almost insensitive to such detection. We understand this discrepancy as follows. Taking the second harmonic as an example, the first partial wave has an amplitude  $\propto t_1 e^{i\chi_1}$ , while the second partial wave  $\propto t_2 e^{i\chi_2} \cdot t_1^* e^{i\tilde{\chi}_1} \cdot t_2 e^{i\tilde{\chi}_2}$ . Here, we formally denote the transmission amplitude through dot-1(2) by  $t_{1(2)}$ , which is in general complex, e.g., containing the Aharonov-Bohm phase;  $\chi_{1(2)}$  and  $\tilde{\chi}_{1(2)}$  are the random phases caused by the charge detection when the electron passes through dot-1(2) in the first- and second-order trajectory.

In Ref. 6, the argument leading to no (or weak) dephasing of the second-harmonic amplitude was based on the assumption that  $\chi_1 \simeq \tilde{\chi}_1$ , together with  $\chi_2 = \tilde{\chi}_2 = 0$  since there is no quantum dot in that arm. Nevertheless, in the DD setup,  $\chi_2 \neq \tilde{\chi}_2 \neq 0$  and  $\chi_1 \neq \tilde{\chi}_1$  in general, because of the time delay between the two partial waves when arriving at the (same) dot. Therefore, the nearby charge detection should dephase the higher order interference trajectories, as shown in Fig. 3(C). In this context, also of very interesting is the phase shift  $\beta_n$ , still satisfying  $\beta_n = n\beta_1$ , even in the presence of dephasing. Numerical result is shown in Fig. 3(D).

*Conclusion.*— We have studied the electron transport through parallel quantum dots, with highlight of the phase shift of the interference pattern which is induced by the interplay of inter-dot Coulomb correlation and quantum coherence. In particular, a harmonic decomposition study for the pattern reveals unexpected behavior of the phase shifts. Dephasing effect is made connection with the information gain of the individual harmonics in the which-path detection, while electron loss is investigated in relation to the conventional double-slit interference.

*Acknowledgments.*— This work was supported by the National Natural Science Foundation of China under grants No. 60425412 and No. 90503013, and the Major State Basic Research Project under grant No.2006CB921201.

- 
- [1] R. P. Feynman, R. B. Leighton, and M. Sands, *The Feynman Lectures on Physics, Vol. III, Chap. 1.* (Addison-Wesley, Reading, 1970).
- [2] G. Hackenbroich, Phys. Rep. **343**, 463 (2001).
- [3] A. Yacoby, M. Heiblum, D. Mahalu, and H. Shtrikman, Phys. Rev. Lett. **74**, 4047 (1995).
- [4] E. Buks *et al.*, Nature (London) **391**, 871 (1998).
- [5] A. Aharony, O. Entin-Wohlman, B.I. Halperin, and Y. Imry, Phys. Rev. B **66**, 115311 (2002).
- [6] D.I. Chang, G.L. Khym, K. Kang, Y. Chung, H.J. Lee, M. Seo, M. Heiblum, D. Mahalu, and V. Umansky, Nature Physics **4**, 205 (2008); G.L. Khym and K. Kang, Phys. Rev. B **74**, 153309 (2006).
- [7] D. Loss and E. V. Sukhorukov, Phys. Rev. Lett. **84**, 1035 (2000).
- [8] E.V. Sukhorukov, G. Burkard, and D. Loss, Phys. Rev. B **63**, 125315 (2001).
- [9] J. König and Y. Gefen, Phys. Rev. Lett. **86**, 3855 (2001); Phys. Rev. B **65**, 045316 (2002).
- [10] M. Sigrist *et al.*, Phys. Rev. Lett. **96**, 036804 (2006).
- [11] A.W. Holleitner *et al.*, Phys. Rev. Lett. **87**, 256802 (2001); A.W. Holleitner *et al.*, Science **297**, 70 (2002).
- [12] Z. T. Jiang, J. Q. You, S. B. Bian, and H. Z. Zheng, Phys. Rev. B **66**, 205306(2002).
- [13] F. Li, X.Q. Li, W.M. Zhang, and S. Gurvitz, arXiv:0803.1618.
- [14] S.-K. Wang, H. Jiao, F. Li, X.-Q. Li, and Y. J. Yan, Phys. Rev. B **76**, 125416 (2007).
- [15] M. Büttiker, Phys. Rev. B **33**, 3020 (1986); IBM J. Res. Dev. **32**, 63 (1988).
- [16] S.A. Gurvitz and Ya.S. Prager, B **53**, 15932 (1996); S.A. Gurvitz, Phys. Rev. B **57**, 6602 (1998).
- [17] X. Q. Li, P. Cui, and Y. J. Yan, Phys. Rev. Lett. **94**, 066803 (2005).
- [18] J. Y. Luo, X.-Q. Li, and Y. J. Yan, Phys. Rev. B **76**, 085325 (2007).
- [19] M. Büttiker, Phys. Rev. Lett. **57**, 1761 (1986);